J|A|C|S
ARTICLES

Published on Web 03/08/2010

Proteins as Electronic Materials: Electron Transport through Solid-State Protein Monolayer Junctions

Izhar Ron,[†] Lior Sepunaru,[†] Stella Itzhakov,[†] Tatyana Belenkova,[†] Noga Friedman,[‡] Israel Pecht,*[,§] Mordechai Sheves,*[,‡] and David Cahen*[,†]

Departments of Materials and Interfaces, Organic Chemistry, and Immunology, Weizmann Institute of Science, POB 26, Rehovot 76100, Israel

Received August 30, 2009; E-mail: david.cahen@weizmann.ac.il

Abstract: Electron transfer (ET) through proteins, a fundamental element of many biochemical reactions, is studied intensively in aqueous solutions. Over the past decade, attempts were made to integrate proteins into solid-state junctions in order to study their electronic conductance properties. Most such studies to date were conducted with one or very few molecules in the junction, using scanning probe techniques. Here we present the high-yield, reproducible preparation of large-area monolayer junctions, assembled on a Si platform, of proteins of three different families: azurin (Az), a blue-copper ET protein, bacteriorhodopsin (bR), a membrane protein-chromophore complex with a proton pumping function, and bovine serum albumin (BSA). We achieve highly reproducible electrical current measurements with these three types of monolayers using appropriate top electrodes. Notably, the current−voltage ($I-V$) measurements on such junctions show relatively minor differences between Az and bR, even though the latter lacks any known ET function. Electron Transport (ETp) across both Az and bR is much more efficient than across BSA, but even for the latter the measured currents are higher than those through a monolayer of organic, C18 alkyl chains that is about half as wide, therefore suggesting transport mechanism(s) different from the often considered coherent mechanism. Our results show that the employed proteins maintain their conformation under these conditions. The relatively efficient ETp through these proteins opens up possibilities for using such biomolecules as current-carrying elements in solid-state electronic devices.

Introduction

Electron transfer (ET) is one of the most fundamental processes in biological systems,[1] crucial for various biological energy conversion processes, from respiration to photosynthesis, and prominent in diverse metabolic cycles. ET reactions are performed by a range of proteins (with specific components that evolved for that purpose) in which electron tunneling occurs over long distances.[2] While these reactions proceed in proteins in their natural, usually aqueous environment, there have been attempts to explore the electronic conductance of various proteins in both wet electrochemical and solid-state configurations. Such efforts mainly used scanning probe microscopy (scanning tunneling microscopy (STM) and conductive-probe atomic force microscopy (CP-AFM)).[3−12] Attempts were also made to integrate proteins into solid-state devices.[13−17] In most of these studies device design was dictated by a biomimetic approach: namely, proteins were expected to conduct current in such metal−protein−metal electrical junctions through pathways similar to those known to dominate the ET process in solution. According to this notion, proteins without redox activity are expected to behave merely as insulators in such electrical junctions.

[†] Department of Materials and Interfaces.
[‡] Department of Organic Chemistry.
[§] Department of Immunology.

(1) Marcus, R. A.; Sutin, N. *Biochim. Biophys. Acta* **1985**, *811* (3), 265–322.
(2) Winkler, J. R.; Di Bilio, A. J.; Farrow, N. A.; Richards, J. H.; Gray, H. B. *Pure Appl. Chem.* **1999**, *71* (9), 1753–1764.
(3) Axford, D. N.; Davis, J. J. *Nanotechnology* **2007**, *18* (14), .
(4) Casuso, I.; Fumagalli, L.; Samitier, J.; Padros, E.; Reggiani, L.; Akimov, V.; Gomila, G. *Nanotechnology* **2007**, *18* (46), 465503.
(5) Delfino, I.; Bonanni, B.; Andolfi, L.; Baldacchini, C.; Bizzarri, A. R.; Cannistraro, S. *J. Phys.: Condens. Matter* **2007**, *19* (22), .
(6) Lee, I.; Lee, J. W.; Greenbaum, E. *Phys. Rev. Lett.* **1997**, *79* (17), 3294–3297.
(7) Reiss, B. D.; Hanson, D. K.; Firestone, M. A. *Biotechnol. Prog.* **2007**, *23* (4), 985–989.
(8) Stamouli, A.; Frenken, J. W. M.; Oosterkamp, T. H.; Cogdell, R. J.; Aartsma, T. J. *FEBS Lett.* **2004**, *560* (1−3), 109–114.
(9) Zhao, J. W.; Davis, J. J.; Sansom, M. S. P.; Hung, A. *J. Am. Chem. Soc.* **2004**, *126* (17), 5601–5609.
(10) Ron, I.; Friedman, N.; Cahen, D.; Sheves, M. *Small* **2008**, *4* (12), 2271–2278.
(11) Alessandrini, A.; Corni, S.; Facci, P. *Phys. Chem. Chem. Phys.* **2006**, *8* (38), 4383–4397.
(12) Friis, E. P.; Andersen, J. E. T.; Kharkats, Y. I.; Kuznetsov, A. M.; Nichols, R. J.; Zhang, J. D.; Ulstrup, J. *Proc. Natl. Acad. Sci. U.S.A.* 1999, *96*, (4), 1379−1384.
(13) Carmeli, I.; Frolov, L.; Carmeli, C.; Richter, S. *J. Am. Chem. Soc.* **2007**, *129* (41), 12352–12353.
(14) Das, R.; Kiley, P. J.; Segal, M.; Norville, J.; Yu, A. A.; Wang, L. Y.; Trammell, S. A.; Reddick, L. E.; Kumar, R.; Stellacci, F.; Lebedev, N.; Schnur, J.; Bruce, B. D.; Zhang, S. G.; Baldo, M. *Nano Lett.* **2004**, *4* (6), 1079–1083.
(15) Maruccio, G.; Biasco, A.; Visconti, P.; Bramanti, A.; Pompa, P. P.; Calabi, F.; Cingolani, R.; Rinaldi, R.; Corni, S.; Di Felice, R.; Molinari, E.; Verbeet, M. R.; Canters, G. W. *Adv. Mater.* **2005**, *17* (7), 816–822.
(16) Mentovich, E. D.; Belgorodsky, B.; Kalifa, I.; Cohen, H.; Richter, S. *Nano Lett.* **2009**, *9* (4), 1296–1300.
(17) Maruccio, G.; Marzo, P.; Krahne, R.; Passaseo, A.; Cingolani, R.; Rinaldi, R. *Small* **2007**, *3* (7), 1184–1188.

However, in earlier work of ours we found that a protein such as bacteriorhodopsin (bR), which has a proton pumping function, i.e., different from ET, is able to mediate electronic transport (ETp) efficiently, if integrated into a metal−protein−metal solid-state junction. In that configuration it was shown to pass currents that are higher than those predicted for a protein of its size.[18] Therefore, the question of what are the *parameters that determine the electronic conductance of proteins in solid-state junctions is an open and intriguing one*.

To pursue these issues, we set out to design the preparation of solid-state protein monolayer junctions, to carry out reproducible ETp measurements that would allow comparative analysis of the results. The strategy for making high-quality monolayer junctions is to use, for each protein, as similar a chemical modification of a conductive substrate as possible and to allow self-assembly of the proteins on the modified surfaces. An additional requirement is to use a nondestructive method for making the top electrical contact to the soft biological monolayer. To try and identify the above-noted parameters, we made a first, comparative study and chose three functionally different protein systems: (1) azurin (Az), a small, soluble, bacterial type 1 blue copper protein, serving as an electron carrier.[19] (2) bacteriorhodopsin, a membrane protein−chromophore complex that functions as a light-induced proton pump, i.e., an electroactive function, in the halophilic archaea, *Halobacterium salinarum*,[20] and (3) bovine serum albumin (BSA),[21] a plasma protein, known to bind and transport a range of hydrophilic molecules and which is readily adsorbed to surfaces. BSA has no known electroactive function. As a non-protein reference that can be measured under the same conditions, we use a monolayer of 18-carbon saturated alkyl chain molecules, which is expected to behave as a molecular tunneling barrier.

In the second part of this paper, we describe the preparation and electrical behavior of modified protein monolayers associated with the three above families, in pursuit of identifying specific chemical components that are crucial for ETp through these proteins.

Results

Protein Monolayer Preparation. The preparation of solid-state protein monolayer junctions is a three-step procedure. First a thin silicon oxide (SiO_x) layer is grown from an oxidizing solution on an etched surface of highly doped Si. We chose Si as substrate because it provides a highly reproducible flat surface, and by using highly doped p-Si it serves as an electrode with minimal semiconductor-related effects. Next, a short bifunctional linker molecule is used to form a monolayer, sufficiently dense to control the tunneling through it (and not through defects, which would be the case if some SiO_x surface were inadvertently exposed to the top electrode), and to allow the proteins to cover the surface completely. Finally, proteins are adsorbed from aqueous solutions by immersing the chemically modified substrates in the protein solutions for times depending on the type of protein−linker bond that is used for the formation of the monolayer. A schematic presentation of this process is shown in Figure 1. The long organic monolayer was assembled from octadecyltrimethoxysilane molecules (OTMS) on top of the oxidized Si. Three types of linker molecules (all of similar length) were used for interaction with the proteins: viz., an *n*-propylsilane chain terminated by an amine, a bromide, or a thiol group.

Az has a disulfide bridge at its surface (on the opposite end of the Cu site), which is commonly used as an anchoring unit to Au surfaces. Az molecules were covalently linked to the thiol- and bromide-terminated surfaces, presumably by means of S−S bond formation or by substitution of the Br group, respectively, yielding identical results in terms of thickness and morphology of the monolayers, and very similar electrical transport characteristics (Az did not bind to the amine-terminated substrate).

Bacteriorhodopsin embedded in vesicles was adsorbed electrostatically on amine-terminated substrates, as its vesicles are negatively charged on both sides, with the cytoplasmic side being more negative.[22] The mixed protein−lipid monolayer formed from native bR protein and lipids,[23] which underwent vesicle fusion upon adsorption.

BSA was adsorbed on each of the three types of substrates by immersing the substrates in its solution. Because BSA is known to adhere to most surfaces, we cannot conclude at this point which group of the protein actually anchors it to each surface, but we assume that the BSA aligns with its major axis parallel to the surface (see below).

Monolayer Surface Characterization. Ellipsometry measurements were carried out on all samples after each preparation step: i.e., oxide growth, silane monolayer formation, and protein monolayer formation. The thickness, deduced from the ellipsometry results, from reported crystallographic dimensions of the proteins and from the results of surface roughness analysis by atomic force microscopy (AFM) imaging are summarized in Table 1. The ellipsometry results, if used in combination with AFM characterization, help to judge if a dense, homogeneous monolayer was obtained, as will be explained later. In all samples the Si oxide layer was 11−12 Å thick, and the silane monolayer thickness was 6−7 Å. Ellipsometry data for the organic and protein layers were analyzed with a Cauchy model.

Az monolayer thickness was deduced from ellipsometry to be 14−18 Å. This agrees with values reported for Az monolayers, derived from ellipsometry and X-ray photoemission spectroscopic (XPS) data. Those values were supported by a theoretical model that simulated the thickness of a layer of barrel-shaped globules with the size of the Az molecules, taking into account the voids that exist between them, if adsorbed on a planar surface.[24] We note that the thickness evaluated by ellipsometry for both Az and BSA (shown below) depends on the model used and may, under certain assumptions, reach (higher) values that are even closer to the estimated molecular dimensions (see the Supporting Information). In the case of Az, the errors in the height estimates from ellipsometry and AFM (see also Figure S7 in the Supporting Information) are such that we cannot rule out the possibility that the protein is aligned with a non-zero angle between the plane of the surface and its

(18) Jin, Y. D.; Friedman, N.; Sheves, M.; He, T.; Cahen, D. *Proc. Natl. Acad. Sci. U.S.A.* 2006, *103*, (23), 8601−8606.
(19) Adman, E. T., *Topics in Molecular and Structural Biology: Metalloproteins*; Chemie Verlag: Weinheim, Germany, 1985; p 1−42.
(20) Oesterhelt, D.; Stoeckenius, W. *Nature (London), New Biol.* **1971**, *233*, 149–154.
(21) Peters, J.; Peters, T. J., *All About Albumin: Biochemistry, Genetics and Medical Applications*; Academic: San Diego, CA, 1995.
(22) He, T.; Friedman, N.; Cahen, D.; Sheves, M. *Adv. Mater.* **2005**, *17* (8), 1023–1027.
(23) Jin, Y. D.; Friedman, N.; Sheves, M.; Cahen, D. *Adv. Funct. Mater.* **2007**, *17* (8), 1417–1428.
(24) Schnyder, B.; Kotz, R.; Alliata, D.; Facci, P. *Surf. Interface Anal.* **2002**, *34* (1), 40–44.

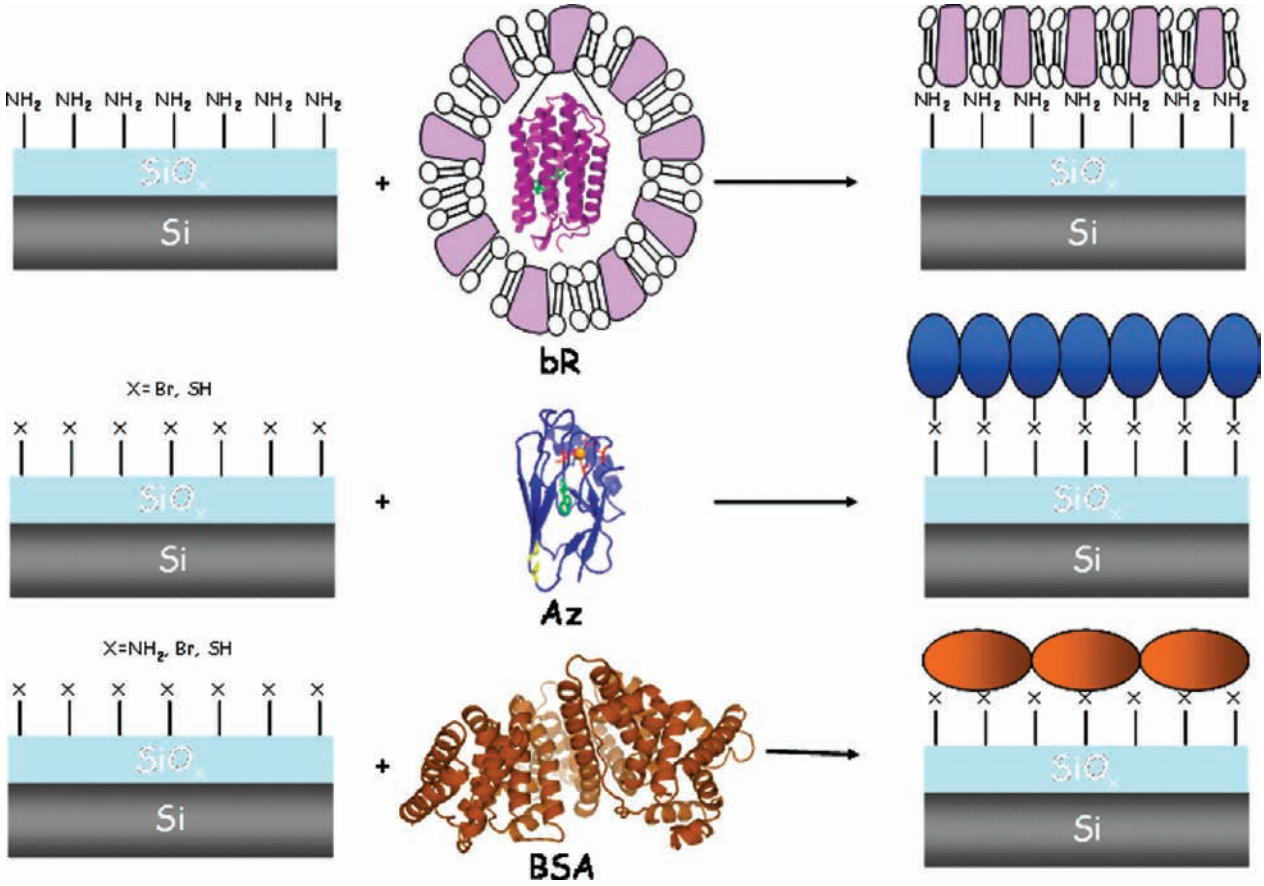

Figure 1. Schematic representation of preparation of protein monolayers, showing bR monolayers (top), Az monolayers (middle), and BSA monolayers (bottom). Coordinates were taken from the Protein Data Bank (PDB): code 1AZU for Az; code 1R2N for bR. The BSA model was obtained from ModBase.

Table 1. Surface Characterization Parameters after All Preparation Stages, for the Monolayers Used in This Study

	ellipsometry-derived thickness, Å	crystallographic/theoretical size (⊥ to surface), Å	rms roughness, from AFM, Å
SiO_x	11−12		2.0
organo-silane (NH_2, Br, SH end groups)	6−7	7	2.5
OTMS	22−25	24	
bR on NH_2	75−80	50−55	
Az on SH or Br	14−18	36	4.0−4.5
BSA on NH_2, SH, or Br	14−18, 20−22, 16−20	40	5.5−6.0

shorter axis; the angle at which it is aligned may influence the electronic transport characteristics.[25]

bR monolayer thickness was calculated from ellipsometry data to be 75−80 Å, significantly longer than the height (∼50−55 Å) of the purple membrane, (which is also the height of the bR protein embedded therein), as measured from coordinates of the bR structure (Protein Data Bank, code 1R2N). This difference may originate in the form of the purple membranes used in the present study, i.e., vesicles that are formed by partial delipidation of the native membranes with a detergent (OTG; see Materials and Methods). Because we find that the optical properties of these vesicles are retained (see below), the difference is likely due to a geometrical change of the lipid−protein structure and not to a change in the structure of the protein, in which case the optical properties would have been altered. As will be shown below, AFM topography of the (solid-supported) fused vesicles also reveals this larger than expected thickness.

The BSA layer thickness was 14−18 Å on the NH_2-terminated surface, 16−20 Å on the Br-terminated surface and 20−22 Å on the SH-terminated surface. BSA dimensions, according to models, are 40 × 40 × 140 Å, which represents an ellipsoidal shape.[21] The measured thickness, within the aforementioned model of a porous macromolecule used for Az, and our AFM characterization (see also Figure S7 in the Supporting Information) allow us to describe the BSA as a barrel-shaped structure, aligned on the surface with its minor axes perpendicular to the surface.[26] The variation in BSA monolayer thickness on substrates with different end groups may result from anchoring by different protein residues, which may lead to slight variations in the orientation in which it is adsorbed. OTMS thickness by ellipsometry was 22−24 Å, in keeping with the size of the molecule, calculated from its 3D structure.

AFM, performed in the Tapping Mode, which is ideal for imaging soft, solid-supported layers, served to examine the morphology of the protein monolayers. The results also

(25) Anurag Setty, V.; Stefano, C.; Rosa Di, F. *Small* **2007**, *3* (8), 1431–1437.

(26) Mori, O.; Imae, T. *Colloids Surf. B: Biointerfaces* **1997**, *9* (1−2), 31–36.

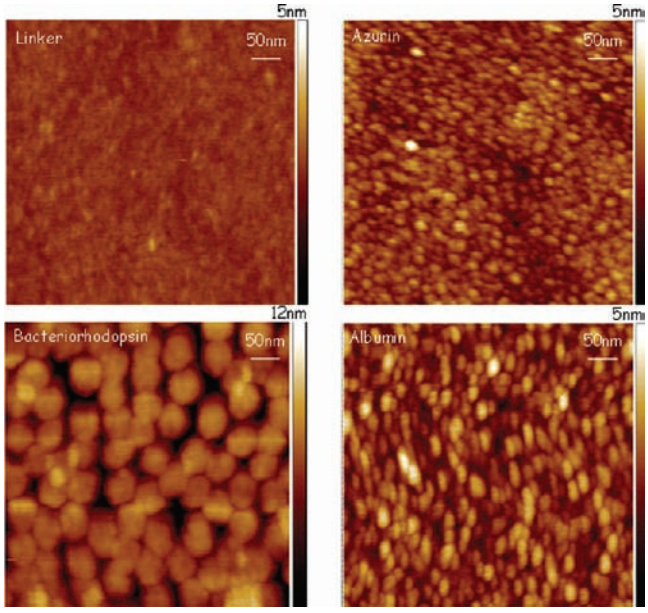

Figure 2. AFM topography images (500 nm × 500 nm) of the OTMS monlayer (top left), Az monolayer (top right), bR monolayer (bottom left), and BSA monolayer (bottom right).

complemented ellipsometry. From AFM imaging, two main features can be deduced. First, the lateral and vertical dimensions of the adsorbed species can be obtained from the image itself and from height profiles, respectively. The second approach, useful in cases where the proteins are too closely packed to evaluate their full height by scanning probe (as is the case of Az and of BSA, see below), is based on the rms roughness of the imaged surface. Figure 2 shows typical AFM height images of the three types of protein monolayers and the organic linker monolayer.

In the Az monolayer, small globular features, covering the surface, are observed (Figure 2, top right). Such features are not observed on the silane monolayer surfaces (Figure 2, top left). The apparent lateral diameter of one globular particle in the AFM image is 170−200 Å, which corresponds to an actual size of ∼ 36−50 Å, taking into account tip−sample convolution.[27] The rms roughness of this surface is 4−4.5 Å, which is only slightly higher than that of the silane-modified SiO_x surface (2.5 Å) and of the bare SiO_x surface (2 Å). This indicates that the Az molecules are densely packed, and, therefore, the full height of the protein (36 Å in the proposed orientation) cannot be measured. In order to overcome this difficulty, we measured the height of isolated Az molecules in a diluted Az (sub)monolayer and found values that are much closer (3−3.5 nm) to the geometrical (longest) dimension (see Figure S7 in the Supporting Information). Coverage analysis (using flooding analysis of WSxM software[28]) results in a surface coverage of 98% over a threshold height of 1 nm. Along with the ellipsometry data, we conclude that the Az monolayer is homogeneous and mostly defect-free.

The bR monolayer is made up of similarly sized fused vesicles that are closely spaced on the substrate (Figure 2, bottom left). The height profile indicates that most vesicles are 70−80 Å high, in keeping with the ellipsometry data (Table 1). Surface roughness analysis is, therefore, not relevant in this case, since the actual relevant height may be measured. A likely explanation for the increased thickness of the bR layer, adsorbed by vesicle fusion, may be that the fused vesicles do not lie completely flat on the surface and remain somewhat curved after fusion to the substrate. To test this hypothesis, we performed AFM on the fused vesicles in semicontact Tapping and contact modes. While in semicontact mode lower forces may be exerted on the vesicles, in contact mode a constant and continuous force is exerted on the vesicles (and shear forces also operate), which should help to flatten them, if they are curved originally. Indeed, such behavior is consistent with the height histograms of the two images, which show a typical height of 7.9 nm in semicontact mode and 4.7 nm in contact mode (Figure S1 in the Supporting Information). Coverage analysis results in 90% coverage over a threshold height of 6 nm.

The BSA monolayer exhibited elongated features with an apparent longer dimension measured to be ∼30−36 nm (Figure 2, bottom right), which translates to 11−16 nm after correcting for tip−sample convolution, in agreement with model estimates of the protein's long dimension. Also here the full height could not be measured on the monolayers used for electrical transport, probably for the same reason as for the case of Az. Using the diluted monolayer approach (mentioned above for Az), we were able to measure the height of isolated BSA molecules and found values similar to those expected from the BSA structural model (3.5−4 nm), with the short dimension perpendicular to the surface (see the Supporting Information). The rms roughness was 5.5−6 Å, higher than that of the Az monolayer. This is reasonable if one takes into account the internal changes of height within a single BSA molecule, which are larger than for Az. In this case, the AFM image itself provides a good morphological picture of the arrangement of the BSA molecules on the surface (the relative regularity of which may be due to protein−substrate interaction). Coverage analysis of the AFM data shows ∼95% coverage over a threshold height of 1 nm. Again, in combination with the ellipsometry data, this indicates a homogeneous layer with high coverage of the surface.

An important question that lies at the very basis of this work concerns the condition of the adsorbed proteins, following removal of all but the most tightly bound solvent molecules, in what we have termed here their "dry" state. This is the condition in which a top metal electrode contacts the proteins and current is measured. Clearly, if the proteins lose their native conformation, we cannot use their original biological functions in any way, in discussing the electrical behavior of the protein-based junctions. We studied, therefore, bR and Az in the dry, adsorbed configuration by measuring their UV−visible absorption and fluorescence spectra, which are highly sensitive to changes in the protein's native conformation. For the bR we used monolayers and for Az multilayers, both on transparent glass or quartz substrates. We used Az multilayers because of the much lower molar extinction coefficient of Az ($\varepsilon_{625\ nm} = 5000\ M^{-1}\ cm^{-1}$) compared to that of bR ($\varepsilon_{570\ nm} = 63\ 000\ M^{-1}\ cm^{-1}$). We were able to measure the bR absorbance spectrum using a stack of four glass slides, each having a bR monolayer (assembled through the same surface chemistry as described above for a Si substrate) on each of its sides (total of eight monolayers), mounted on a custom-made holder. The resulting spectrum is shown in Figure 3a, displaying a band around 570 nm, similar to the absorption of the light-adapted bR pigment (formed by the retinal chromophore linkage to the protein) in solution (λ_{max}

(27) Biasco, A.; Maruccio, G.; Visconti, P.; Bramanti, A.; Calogiuria, P.; Cingolani, R.; Rinaldi, R. *Mater. Sci. Eng. C: Biomimetic Supramol. Syst.* **2004**, *24* (4), 563–567.
(28) Horcas, I.; Fernandez, R.; Gomez-Rodriguez, J. M.; Colchero, J.; Gomez-Herrero, J.; Baro, A. M. *Rev. Sci. Instrum.* **2007**, *78*, (1).

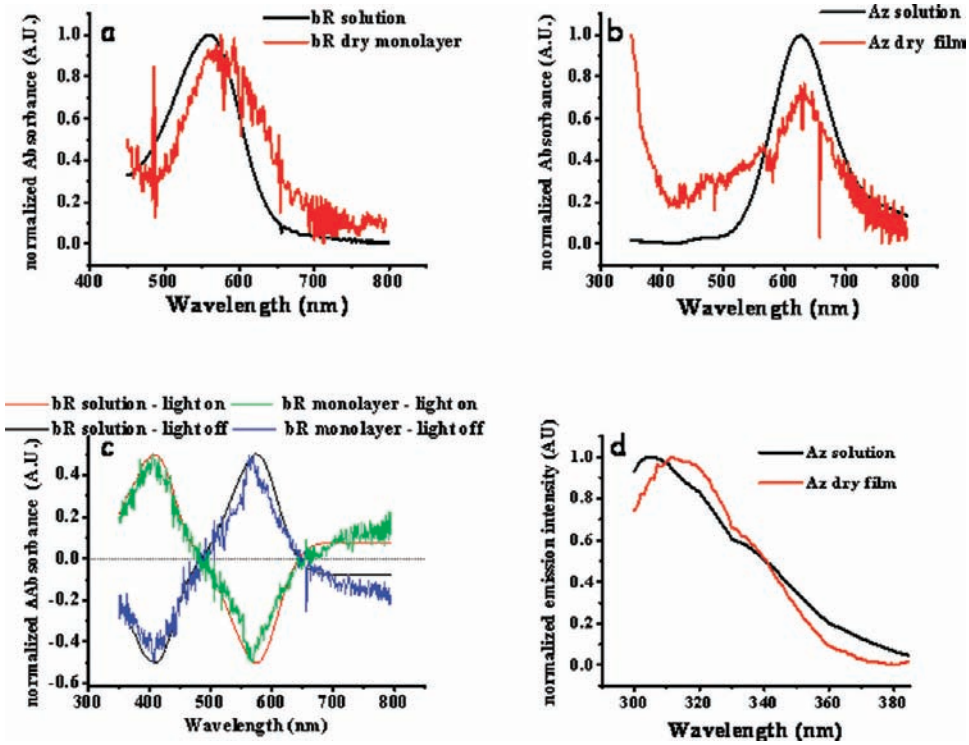

Figure 3. Optical characterization of the dried, solid-supported protein layers: (a) UV−vis absorption spectrum of eight bR monolayers, prepared in the same way as on Si/SiOx, on both sides of four glass slides; (b) UV−vis absorption spectrum of a multilayer of Az molecules, prepared by drying (under vacuum) a drop of Az solution (70 μM) on a glass slide; (c) photoactivity of bR monolayers, as recorded on the same series of monolayers as in (a), showing the difference spectra taken between dark and illumination with yellow (>545 nm) light, and the recovery of the 570 nm band upon turning off the illumination; (d) normalized fluorescence emission spectra of Az solution and of a multilayer of Az on a quartz slide, prepared by drying a drop of Az on the quartz substrate under vacuum. The excitation wavelength was 275 nm.

568 nm). The measured absorption around 570 is OD = 6.7×10^{-3}, corresponding to absorption of 8.4×10^{-4} per monolayer, which is only slightly lower than previous measurements on dry layers of bR.[23,29] We prepared a multilayer of Az by drying a drop of the protein solution (70 μM) on a glass substrate at low vacuum. The resulting spectrum shows a clear band around 625 nm (Figure 3b), corresponding to the optical transition between the Cu^{II} and the thiolate residue of its cysteine ligand. To further characterize the condition of these proteins in the dry, adsorbed state, we studied the photoactivity of bR in the same configuration, used for the absorption spectrum measurement above. As can be seen in the difference spectrum in Figure 3c, upon illumination with $\lambda > 545$ nm, bR switches from the ground state to the M state (λ_{max} 412 nm), and decays back to the ground state after illumination is turned off. This clearly demonstrates that a monolayer of bR in the dry state maintains its normal photoactivity and, therefore, its native structure. In agreement with what we reported earlier,[22] in the dry monolayer the kinetics of the photoactivity are slowed, probably due to a slower M state thermal decay than in solution, as indicated by the accumulation of the M intermediate under continuous illumination (and this is in keeping with the behavior of a M state accumulating bR species; Figure 3c).

Az in the dry state was further characterized by examining the unique emission of the Trp48 residue of Az, at a very short wavelength (308 nm) due to its hydrophobic environment.[30] This fluorescence is very sensitive to the Trp residue environment and can, therefore, serve as a good probe for the conformation of the dried protein as the denatured protein fluoresces at higher wavelength (~340 nm). While the emission of this Trp residue in Az is usually measured in Apo-Az, in order to limit quenching by the Cu(II), we were able to measure the typical fluorescence of the holoprotein, on the same type of multilayer as that used for the UV−vis absorption spectrum. Figure 3d shows the normalized spectra of an Az solution and of the dried Az multilayer on a quartz substrate. No bathochromic shift typical of even a partial denaturation is observed. The slight red shift that is observed was reported also for a similar measurement on Apo-Az.[15] On the basis of these optical characterizations we conclude that both bR and Az maintain their native conformation upon drying (removal of all but the most tightly bound solvent) and adsorption onto a solid support.

Electronic Transport Measurements. ETp measurements were carried out with either a hanging Hg drop[31] or a 60 nm thick "ready-made" Au pad, deposited from water onto the monolayer (Lift Off, Float On(LOFO)),[32] as second electrode/contact. We measured the samples using the two methods separately, so as to eliminate possible effects of a specific metal and contacting method on the junctions' transport characteristics. Because similar results were obtained with both methods, we will refer to the results obtained with the Hg drop top contact only, simply because practically it is easier to collect data with this method than with the Au one. Still, ETp results for Az and bR, obtained with Au *and* Hg top contacts, are shown in Figure

(29) He, J.-A.; Samuelson, L.; Li, L.; Kumar, J.; Tripathy, S. K. *Langmuir* **1998**, *14* (7), 1674–1679.
(30) Grinvald, A.; Schlessinger, J.; Pecht, I.; Steinberg, I. Z. *Biochemistry* **1975**, *14* (9), 1921–1929.
(31) Salomon, A.; Boecking, T.; Chan, C. K.; Amy, F.; Girshevitz, O.; Cahen, D. *Phys. Rev. Lett.* **2005**, *95* (26), 266807.
(32) Vilan, A.; Shanzer, A.; Cahen, D. *Nature* **2000**, *404* (6774), 166–168.

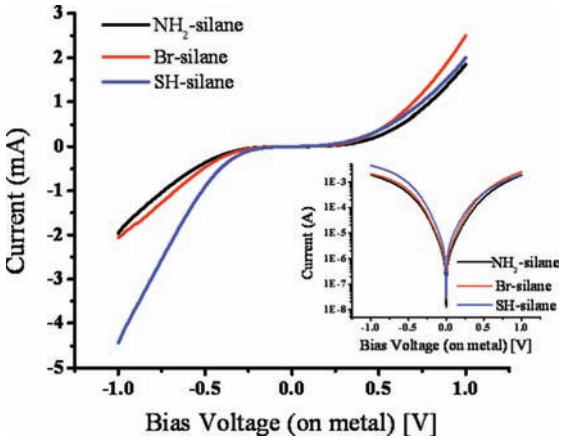

Figure 4. *I*−*V* characteristics of the three silane monolayers (with the three different terminal groups). The inset gives a semilog plot of these results.

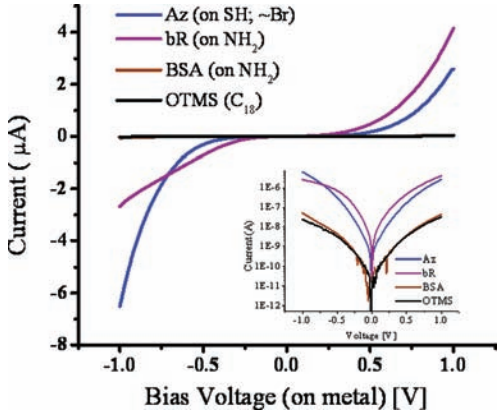

Figure 5. *I*−*V* characteristics of the three protein monolayers and the organic saturated chain (OTMS) monolayer. The inset gives a semilog plot of these results.

S2 (Supporting Information).[33] We calculated that the possible forces exerted on the protein layers by the deposition of these two types of metal contacts are of the same order of magnitude as the forces exerted by the tip in conductive probe AFM measurements (in the latter the forces were especially chosen to make the measurements noninvasive[9]) (see Supporting Information).

Figure 4 shows current−voltage (*I*−*V*) curves of the three different linker monolayers. The current magnitudes, extracted from these curves, will later be used as the initial current entering the protein monolayers that assembled on top of these linker molecules. It is evident that, for all three linkers, the current at ±1 V bias voltage is on the order of mA. The bare SiO_x surface behaves more as an ohmic junction, with current magnitudes of 100 mA (instrument limit) at ±0.4 V, corresponding to ∼4 Ω resistance (Figure S3 in the Supporting Information).

Figure 5 presents *I*−*V* curves of Az on the SH-terminated substrate, bR on NH_2-terminated substrate, BSA on NH_2-terminated substrate (*I*−*V* curves of Az and BSA on Br-terminated substrates are shown in Figure S4 in the Supporting Information), and OTMS on SiO_x. Three trends are apparent from these curves. First, currents through bR and Az monolayers are of the same magnitude; this is surprising, considering the size of bR compared to Az, and more important, bR's lack of any known ET function, as opposed to Az. Second, currents through Az and bR are on the order of μA at ±1 V, while currents through BSA and OTMS are on the order of tens of nA (see semilog plot in Figure 5, inset).[34] The third issue concerns the shape of the *I*−*V* curves. The curves for bR show asymmetry toward positive bias (bias applied on the metallic top contact), while those for Az show asymmetry toward negative bias (asymmetry ratio in both cases is ∼2). The *I*−*V* curve for just the underlying substrate relevant for bR (NH_2-terminated substrate) was almost symmetric, while asymmetry of Az samples was observed with the two different linkers (Br- and SH-terminated substrates), but these two substrates themselves showed opposite asymmetries (slightly positive with Br and negative with SH). We therefore suggest that the observed asymmetry reflects properties of the proteins in the junctions.

The following reasons strongly indicate that ETp occurs through the proteins and not through other routes in the junction:

- the pronounced difference between current magnitude observed with Az and bR, and that with BSA (despite the thickness and coverage analysis presented above)
- the difference in ETp between Az and bR, on the one hand, and OTMS (a much shorter barrier), on the other hand
- the similarity between OTMS and BSA, notwithstanding the large difference in size between them
- the rough similarity between liquid Hg and "ready-made" Au pad contacts[35]
- the much higher currents measured through the linker molecules only

On this basis we will now interpret the observed results.

ETp through Solid-State Protein Junctions. As already noted, currents through Az and bR are of comparable magnitude. Both monolayers attenuate the currents that pass through the underlying linker monolayers, by about 3 orders of magnitude. This result is surprising, as one could naively expect that only an ET protein such as Az would allow efficient ETp through such a junction, while bR should, according to this approach, function as a mere insulator. Already in our earlier work we noted the remarkably efficient ETp through bR[23] but could not put it in perspective. This is now possible by comparing bR ETp with that of two other proteins and an organic molecule, all measured under the same conditions. To quantify the ETp *differences* between the different protein systems employed, we will first

(33) We note that for BSA currents an order of magnitude higher were measured using the LOFO method, in comparison with those for Hg contacts, and this issue is still being studied. One possible explanation is that, unlike Az and bR, BSA is not robust enough to withstand the deposition of a gold film without undergoing partial loss of conformation.

(34) We note here that in our previous work on bR solid-state junctions the observed currents were ∼2 orders of magnitudes lower, for a similar junction area.[14] We attribute this discrepancy to two factors: first, in this previous work the oxide layer was much thicker (oxide grown on Al surface); second, the back contact made now with InGa could not be used on the AlOx surface, and the series resistance then was higher.

(35) In principle the high currents could be due to partial penetration of the metal contact through the protein monolayers, and we cannot rule this out categorically. However, two facts make this an extremely unlikely scenario: the first is the fact that the results with these two different types of contacts are comparable (in terms of current magnitudes and asymmetry); the second is that to consider tunneling through free space as dominating these junctions, taking $\beta \approx 2$ Å^{-1} for free space, the barrier widths that will result in current levels that were measured with Az, bR, and BSA are 3.3, 3, and 5.3 Å, respectively (for the full area of the junction, a case which is not likely in itself if only penetration in between adsorbed molecules is considered).

consider the protein monolayers as simple tunneling junctions, an approach which involves two strongly simplifying assumptions:

(1) Fitting the ETp results to a simple mono-exponential decay, $I = I_0 \exp(-\beta l)$, we can extract a value for *the effective decay* parameter, β. To this end we take the currents that pass through the assembly *without the proteins* as I_0, the currents through junctions with the proteins as I (under an applied bias of ± 1 V, see Table S1 in the Supporting Information), and the protein's crystallographic length, l, as the tunneling barrier width. Extracting a value for β from the monoexponential term allows normalizing charge transport efficiency through junctions with different barrier widths. While this entails the major oversimplified assumption that transport is only by tunneling, it allows some comparison between junctions composed of proteins of different sizes.

(2) Even though the geometrical area is the same for all junctions, the number of molecules per unit area is different, mainly because the three types of proteins are of different sizes. Therefore, the number of molecules contacted by the top electrode and participating in the ETp process is not the same for all protein junctions. However, because at this point we do not know which path(s) the electrons follow in the proteins, we must also consider the possibility that the proteins in these junctions may comprise several conduction pathways.[36] Therefore, *we normalize current to a given area (by using the geometrical surface area of the contact)*, rather than to the number of protein molecules contacted by this area (assuming that conduction pathways are more closely spaced than the sizes of the examined proteins).

From these analyses (Table S1, Supporting Information) $\beta = 0.68$ Å^{-1} for the OTMS monolayer junction was extracted. While our β value should be distinguished from those obtained in the more conventional way (from the slope of a semilog plot of ET rates/conductance vs distance), the value that we obtain does fall within the range of decay constants proposed for tunneling through nonconjugated organic molecules.[37] In any case, the important result is that the three protein-containing junctions yield β values that are significantly lower than 0.68 Å^{-1}, with bR yielding an even lower value (0.12 Å^{-1}) than Az (0.18 Å^{-1}) and BSA giving the highest decay constant among the three proteins (0.27 Å^{-1}). How we can understand that all three proteins, regardless of their functions and possible unique features, display much more efficient ETp than the aliphatic chains, as measured in our system, is a question considered in the Discussion.

ETp on Modified Protein Monolayers. The results presented above indicate that the measured currents flow dominantly through the proteins, which then should allow studying the role of specific groups within the proteins in mediating ETp. In bR and Az, the groups of interest are those which determine the functions of these proteins: namely, the retinal chromophore in bR and the Cu ion in Az.

We prepared bR vesicle suspensions that contain the protein with its chromophore unbound (by cleaving the Schiff base bond), referred to as Apo-bR. In addition we prepared bR vesicle suspensions that contain retinal-free protein (washed Apo-bR). We prepared monolayers from these bR variants with the same procedure as described above for the wild type bR. The ellipsometry and AFM characterization of these monolayers indicated that they are similar to the WT-bR monolayer (Figure S5 in the Supporting Information), which is a necessary requirement for being able to compare between the measured ETp results. Figure 6 shows $I-V$ results of the three bR species. It can be seen that currents through WT-bR and Apo-bR are similar, while currents through washed Apo-bR are dramatically attenuated. This result shows clearly the role of the retinal chromophore in mediating ETp through bR, even in its unbound state. It demonstrates, furthermore, that the measured current is dominated by electron flow through the proteins, rather than through the detergent and native lipids that are still present in the monolayer. These results reproduce, in the present experimental configuration, our previous ones on bR.[18]

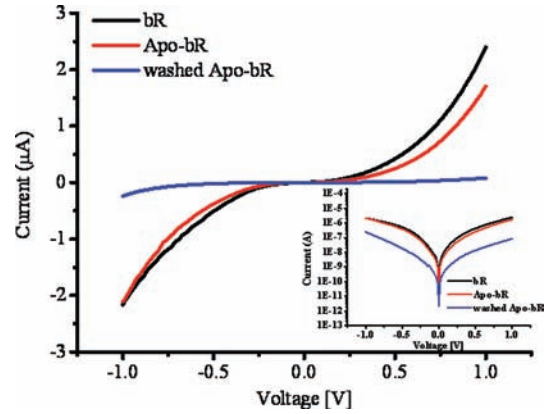

Figure 6. $I-V$ characteristics of the bR monolayers (bR, Apo-bR, and washed Apo-bR). The inset give a semilog plot of these results.

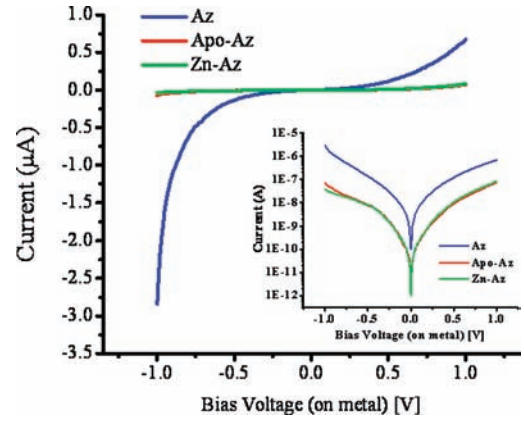

Figure 7. $I-V$ characteristics of the three Az monolayers (Az, Apo-Az, and Zn-Az). The inset gives a semilog plot of these results.

The role of the Cu redox center in Az was studied by measuring ETp through Apo-Az and Zn-Az monolayers, prepared on a thiol-terminated surface by the same procedure as that described above for the holo-Az. Again, our surface characterization yielded similar results for these monolayers with respect to the holo-Az (Figure S6 in the Supporting Information). Figure 7 shows $I-V$ results of the Az variants. Two features are notable from this graph: one is that currents through holo-Az are close to 2 orders of magnitude higher than those measured through both Apo-Az and Zn-Az. This result strongly supports the assumption that the Cu redox center of Az participates in the electron transport also in this solid-state configuration. Upon removal of the redox-active metal ion or replacing it by a redox-inactive one (Zn), the protein behaves

(36) Beratan, D. N.; Onuchic, J. N.; Winkler, J. R.; Gray, H. B. *Science* **1992**, *258* (5089), 1740–1741.
(37) Salomon, A.; Cahen, D.; Lindsay, S.; Tomfohr, J.; Engelkes, V. B.; Frisbie, C. D. *Adv. Mater.* **2003**, *15* (22), 1881–1890.

merely as a protein matrix, displaying a behavior similar to that of the electro-inactive protein BSA, shown in Figure 5. The other feature is the asymmetry observed in the $I-V$ characteristics of holo-Az that is not observed in Apo-Az and Zn-Az (actually, a slight opposite asymmetry is observed in the last two species). The asymmetry reflects the polarity of the Az junction that affects the electrical behavior, probably by the Cu acting as a strong carrier of electrons, injected by the top metal electrode under negative bias voltage. Upon removal of the Cu, or upon its replacement by the redox-inactive Zn^{II}, the I−V characteristic seems more typical to a tunneling barrier, again similar to that shown earlier for BSA and OTMS. This observation implies that without the Cu, electrons travel through different pathways in the protein but less efficiently.

Discussion

An important achievement of this study is that the protein monolayers which we prepared are homogeneously dense and suitable for electrical transport measurements. Indeed, using top electrodes that do not damage the protein monolayers, ETp measurements on these junctions are very reproducible. Dozens of junctions prepared from all the described monolayers, could be measured without the occurrence of short circuit currents (currents that are dominated by pinholes or imperfections in the protein monolayers; cf. Electrical Measurements in Materials and Methods). Therefore, this system can be used reliably to investigate how the different proteins conduct current.

By extracting current values observed at a given voltage and by comparing them with those measured through the same junctions *without* the protein monolayer, we can deduce average effective tunneling decay coefficients of the protein junctions. The possibility of direct tunneling via long separating media such as proteins (several nanometers) is frequently ruled out, and the low decay constants that we extract support the idea that a mechanism different from the one that operates in (mostly optical) measurements of ET in solution[38,39] dominates in solid-state ETp measurements. We suggest that for ETp proteins should not be viewed as providing a simple (single) molecular tunneling barrier as is commonly done for saturated hydrocarbon chains. Rather, it is likely that two (or more) tunneling steps are involved, as already suggested by us for bR.[16] At the same time, the two types of proteins that have charge transport as their biological function (bR and Az) are found to be significantly better conductors than the ET-inactive protein (BSA).

A mechanistic model that is proposed as an alternative to tunneling in molecular bridges is that of inelastic charge *hopping*, where electrons (or holes) travel through the bridge by tunneling steps from one hopping site to the next, in a process that is only weakly dependent on distance.[40] Hopping may be considered to compete with tunneling, depending on the bridge levels' positions, on the bridge length, and on thermal activations.[41] Future ETp measurements as a function of temperature on our systems may help determine the relative importance of these two mechanisms by showing if, and to what extent, the processes that we observe are thermally activated.

For ET within proteins in solution a marked dependence on the distance separating donor and acceptor was observed. We note several differences between ET through proteins in solution and our ETp measurements:

- In solid-state ETp, a bias voltage is applied, which introduces a flow of electrons from and to (infinite) reservoirs (the conducting contacts)
- Under bias a significant electric field exists in the nanometer-sized solid state ETp gap
- In our solid-state ETp configuration we measure current flow across the assumed *full crystallographic dimension* of the relevant protein, which is larger than the length of the path of ET through proteins in solution studies, which allows a single tunneling step

All these differences suggest that while we undoubtedly can learn from solution photo- and electrochemical results, caution is needed when making direct comparisons. Thus, the difference in lengths is possibly what allows us to observe the regime where multistep tunneling dominates in proteins. This difference may help understanding why here we can observe the difference in decay strengths between saturated organic and protein media. As long as single tunneling steps are measured, these two media can be characterized by relatively similar decay parameters. In our longer, probably multistep tunneling junctions, proteins behave differently. Indeed, our results imply that proteins are capable of supporting long-range multistep tunneling. In addition, we observe in the currently employed configuration a strong link between known properties of the bR and Az and their ETp characteristics. The dramatic changes in currents in response to removing or replacing a single cofactor (retinal) or ion (Cu), in the respective protein, in a junction that consists of $\sim 10^{10}$ protein molecules strongly suggest that our approach indeed allows us to resolve the parameters that determine ETp at the molecular level.

As for the more efficient ETp across BSA than across the alkyl chain OTMS, we suggest that this may reflect the additional role of the protein matrix (peptides), which on top of providing a mechanical scaffold and binding the cofactors at fixed distances may also facilitate ET by increasing the electronic coupling along the intercofactor path.

Another indication for a specific role for the proteins in our ETp measurements is the observed asymmetrical transport behavior of both Az and bR junctions, which is uncommon in junctions dominated by coherent tunneling.[42] If, in such junctions, all of the potential drops over the interfaces, the current−voltage curves will usually be symmetrical. Substrate-independent asymmetry is another indication that ETp across Az and bR is sensitive to the chemical nature of the separating medium.

An important issue in these junctions is the role played by water molecules in the ETp process. Assuming that bulk water is not relevant in the presently employed dry state, one is left with only tightly bound water molecules (which are part of the protein's native structure) and the water layer found at the protein's surface. Thus, the role of tightly bound water is not resolved in this study, because in order to remove these, one needs to work under high vacuum, where the structure of the protein may be altered. These water molecules may also be part of the reason for the observed high conductance, even for an electro-inactive protein. Such high conductance may well be an intrinsic property of the protein. The role that bound water molecules as well as water at the protein surface play in affecting

(38) Edwards, P. P.; Gray, H. B.; Lodge, M. T. J.; Williams, R. J. P. *Angew. Chem., Int. Ed.* **2008**, *47* (36), 6758–6765.
(39) Paddon-Row, M. N. *Aust. J. Chem.* **2003**, *56* (8), 729–748.
(40) Jortner, J.; Bixon, M.; Langenbacher, T.; Michel-Beyerle, M. E. *Proc. Natl. Acad. Sci. U.S.A.* 1998, *95*, (22), 12759−12765.
(41) Segal, D.; Nitzan, A.; Davis, W. B.; Wasielewski, M. R.; Ratner, M. A. *J. Phys. Chem. B* **2000**, *104* (16), 3817–3829.
(42) Mujica, V.; Ratner, M. A.; Nitzan, A. *Chem. Phys.* **2002**, *281* (2−3), 147–150.

ETp requires further experiments done at different relative humidities (RH). Such experiments were done in CP-AFM experiments on Az, and the results showed that the resistance changes only slightly ($\leq$10%) in the range of 20−60% RH.[43] For bR it was previously shown that water molecules (tightly bound and as a layer at the surface of the protein) influence the function of the protein and the kinetics of its photocycle.[44−48] While our results (Figure 3) suggested that both Az and bR retained their native structure and optical signatures, experiments at different RH values will be of interest per se and to explore the role of water in ETp.

Notwithstanding such considerable uncertainties, we feel that we can draw our conclusions, thanks to the ability to measure junctions made of different proteins and molecules under the same conditions and to compare the results for different proteins and for a given protein between its holo- and apo-protein states.

This study is the first step toward investigating protein conductivity in the solid state, in a configuration of an ensemble of molecules (and not at the single-molecule level), a configuration that can serve as a template for protein-based devices. Future work will focus on studying the effect of point mutations of specific amino acids; Trp, for example, present in Az and bR, is one appealing candidate, considering its known role in facilitating ET in proteins.[49,50]

Conclusions

We have described the highly reproducible preparation of solid-state protein monolayer junctions, containing three distinct types of proteins, and provided characterizations which indicate that proteins maintain their native conformation upon removal of solvent (to the extent of leaving only the tightly bound water molecules) and that, therefore, the role of their structure/function can be considered when interpreting their electronic transport behavior. We demonstrated high-yield electrical transport measurements on these junctions. Our results clearly show that even a system that does not function as an electron carrier (bR) can facilitate electronic current flow in the solid state; another result supports the dominant role of the retinal chromophore in bR in this process, which we postulated earlier,[18] and the role of the Cu ion in Az. The electrical charge transporting proteins (Az and bR) seem to provide more efficient ETp than a protein such as BSA that has no known electrical charge transport function. Still, a BSA-containing monolayer shows ETp efficiency higher than a monolayer made up of simple saturated organic molecules (OTMS).

ETp across the proteins cannot be interpreted by the simple coherent tunneling model that is commonly used for junctions containing an organic molecular monolayer. A sequential inelastic transport model seems more likely at this stage, and future work shall deal with the temperature dependence of ETp. We hope that our preparation and measurement methods can serve as a general platform for studying ETp across proteins in a solid-state configuration. The remarkable current densities (on the order of mA/cm^2) that were measured indicate that proteins should not be viewed as insulators. The observed electronic current dependence on some of the protein's functionalities may help building a basis for protein-based electronic devices.

Materials and Methods

Monolayer Preparation. Highly doped (<0.005 Ω cm) p-type silicon wafers ⟨100⟩ were cleaned by bath sonication in ethyl acetate/acetone/ethanol (2 min in each), followed by 30 min of piranha treatment (7/3 v/v of H_2SO_4/H_2O_2) at 80 °C. The wafers were then thoroughly rinsed in Milli-Q (18 MΩ) water, dipped in 2% HF solution for 1 min in order to etch the Si surface (leaving a Si−H surface), and put in fresh piranha for 25 min for controlled growth of the oxide layer. After this step, the wafers were thoroughly rinsed in water and dried under a nitrogen stream. The resulting SiO_x layers served as a substrate for preparation of three different organo-silane layers:

(1) A (3-aminopropyl)trimethoxysilane (3-APTMS, NH_2-terminated linker, Aldrich) monolayer was prepared by immersing the SiO_x substrate in 10% v/v 3-APTMS in methanol for 3 h, followed by 3 min of bath sonication in methanol and rinsing in water.

(2) (3-Bromopropyl)trichlorosilane (3-BPTCS, Br-terminated linker, Aldrich) monolayers were prepared by immersing the SiO_x substrate in 10 mM 3-BPTCS in bicyclohexyl (BCH) for 30 s, followed by 2 min of bath sonication in toluene and rinsing in ethanol.

(3) (3-Mercaptopropyl)trimethoxysilane (3-MPTMS, SH-terminated linker, Fluka) monolayers were prepared by immersing the SiO_x substrate in 10 mM 3-MPTMS in bicyclohexyl (in the presence of 5 mM DTT) overnight, followed by 2 min of bath sonication in acetone and rinsing in ethanol.

(4) OTMS (octadecyltrimethoxysilane) monolayers were prepared by immersing the SiO_x substrate in 10 mM OTMS in bicyclohexyl overnight, followed by sonication for 2 min in acetone and rinsing in ethanol.

Proteins. For *bacteriorhodopsin*, a suspension of purple membrane fragments containing wild-type bR was prepared by a standard method.[51] Membrane vesicles were prepared by following the procedure of Kouyama et al.[52] This method involves partial delipidation of the native membrane fragments with a mild detergent, octylthioglucoside (OTG). This bR preparation will therefore be referred to as bR-OTG.

bR-OTG was bleached in the presence of 2 M NH_2OH (pH 9.2) and dialyzed against a solution of 0.01 M phosphate buffer (pH 6.4) and 0.1 M ammonium sulfate. In order to wash out retinal oxime, a suspension of Apo-OTG ($C = 1 \times 10^{-5}$ M, 1 mL) and *n*-hexane (1.3 mL) was sonicated (2 min) and centrifuged and the layers were separated. The same procedure was repeated four additional times, resulting in washed-apo-OTG.

Azurin was isolated from *Alcaligenes faecalis* by the method of Ambler and Wynn.[53]

A280/A625 values of the isolated and purified protein were ~2.0.

Apo-Az was prepared by overnight dialysis of 2−3 mL of Az against 1 L of 0.1 M KCN (pH 7, adjusted with acetic acid). The dialysis was repeated until no blue color was observed. The cyanide was removed by dialysis against ammonium acetate (0.05 M, pH 7).

Substitution of copper ion in Az with Zn^{2+} was done in a way similar to Co substitution.[54,55] Zn-Az was prepared by adding two

(43) Davis, J. J.; Wang, N.; Morgan, A.; Zhang, T. T.; Zhao, J. W. *Faraday Discuss.* **2006**, *131*, 167–179.
(44) Rousso, I.; Friedman, N.; Lewis, A.; Sheves, M. *Biophys. J.* **1997**, *73* (4), 2081–2089.
(45) Papadopoulos, G.; Dencher, N. A.; Zaccai, G.; Buldt, G. *J. Mol. Biol.* **1990**, *214* (1), 15–19.
(46) Varo, G.; Lanyi, J. K. *Biophys. J.* **1991**, *59* (2), 313–322.
(47) Varo, G.; Keszthelyi, L. *Biophys. J.* **1983**, *43* (1), 47–51.
(48) Korenstein, R.; Hess, B. *Nature* **1977**, *270* (5633), 184–186.
(49) Shih, C.; Museth, A. K.; Abrahamsson, M.; Blanco-Rodriguez, A. M.; Di Bilio, A. J.; Sudhamsu, J.; Crane, B. R.; Ronayne, K. L.; Towrie, M.; Vlcek, A.; Richards, J. H.; Winkler, J. R.; Gray, H. B. *Science* **2008**, *320* (5884), 1760–1762.
(50) Farver, O.; Pecht, I. *J. Am. Chem. Soc.* **1992**, *114* (14), 5764–5767.
(51) Oesterhelt, D.; Stoeckenius, W. *Methods Enzymol.* **1974**, *31* (Pt A), 667–678.
(52) Denkov, N. D.; Yoshimura, H.; Kouyama, T.; Walz, J.; Nagayama, K. *Biophys. J.* **1998**, *74* (3), 1409–1420.
(53) Ambler, R. P.; Wynn, M. *Biochem. J.* **1973**, *131* (3), 485–498.
(54) Tennent, D. L.; McMillin, D. R. *J. Am. Chem. Soc.* **1979**, *101* (9), 2307–2311.

to five equivalents of $Zn(CH_3COO)_2 \cdot 2H_2O$ to the apo protein and allowing to stand for two to three days at room temperature. Then the excess ions were removed by dialysis.

BSA was prepared by dissolving Fraction V powder (SIGMA) in buffer solution.

Protein Monolayers. *Bacteriorhodopsin* monolayers and modified bR monolayers were prepared by immersing the NH_2-terminated substrates in a bR vesicle suspension for 15 min followed by transferring the sample to water and keeping it for 3 h to allow vesicle fusion. After the substrates were taken out, they were gently rinsed in water and dried under a fine nitrogen stream.

Azurin monolayers and modified Az monolayers were prepared by immersing the SH- and Br-terminated substrates in a 1 mg/mL solution of azurin in 50 mM ammonium acetate (NH_4Ac) buffer (pH 4.6) for 3 h followed by rinsing in clean 50 mM NH_4Ac buffer and finally in H_2O, followed by drying under a fine nitrogen stream.

BSA monolayers were prepared by immersing the NH_2-, Br-, and SH-terminated substrates in 1 mg/mL solutions of BSA in 20 mM phosphate buffer (pH 7) for 2 h followed by rinsing in clean 20 mM phosphate buffer and finally in H_2O, followed by drying under a fine nitrogen stream.

Back Contacts. Before the electrical transport measurements, the back sides of all samples were scratched with a diamond pen and In−Ga eutectic was applied to the back of the sample. The samples were mounted on a conducting sample holder.

Top Metal Electrode Deposition. Au pads (60 nm thickness, 0.5 mm diameter) were evaporated on clean glass slides. The pads were lifted off the glass slide by immersing them in 2% HF solution and then dipping in H_2O, to allow the pads to float on the water surface. Samples were dipped into the water and pulled out until a pad was deposited on the surface. After several pads were deposited on each sample, the sample was left to dry overnight under ambient conditions. During the measurements these contacts were contacted by a 35 μm wide Au wire that was attached to a W probe, mounted on a micromanipulator.

Hg drop top contacts were applied by placing a Hg drop (99.9999% purity) on the monolayer, using a controlled growth hanging mercury drop (HMD) electrode apparatus (Polish Academy of Sciences). The samples were mounted on a conducting sample holder whose position was controlled by a micromanipulator. The geometrical contact areas of the Au and Hg contacts were 0.002 and 0.002 ± 0.0005 cm^2, respectively.

Electrical Measurements. *I*−*V* curves were measured on samples from at least three different preparations. In each preparation at least two separate samples (of each type) were measured. The Hg drop was used to contact 10 points on each sample, which was 8 × 12 mm in size. Before and after the measurement of each sample, and after every few spots on the sample, the Hg drop was used to measure a reference sample. *Current*−*voltage (I*−*V)* characteristics that are shown are the average of at least 60 different junctions, on three different sample preparations for each type of protein. The standard error of this averaging is less than 10%. Short circuit junctions were observed in less than 5% of the measurements.

Instruments. *Ellipsometry* measurements were performed with a Woollam M-2000 V multiple-wavelength ellipsometer at an angle of incidence of 70°.

AFM imaging was performed in the tapping mode, using a Nanoscope V Multimode AFM (Veeco) and standard Si probes for AC mode AFM (OMCL-AC240TS-W2, Olympus).

Current−*voltage (I*−*V)* measurements were performed using a Keithley 6430 subfemtoamp source meter, with a voltage scan rate of 20 mV/s.

UV−*visible absorption* spectra were recorded using an HP 8453 diode array spectrophotometer.

Fluorescence spectra were recorded using a Fluorolog-3 fluorimeter (HORIBA Jobin Yvon).

Acknowledgment. We thank Prof. Mati Fridkin (WIS) for advice on protein adsorption, Dr. Sidney R. Cohen and Dr. Einat Tirosh (WIS) for help with AFM experiments and calculations, Eyal Capua and Royi Kaufmann (WIS) for help with the organosilane protocols, Tal Honig and Gilad Gotesman (WIS) for help with fluorescence measurements, and Tali Aqua (WIS) for help with ellipsometry. Partial support from the NATO Science for Peace Program (D.C.), the Nancy and Stephen Grand Centre for Sensors and Security (D.C.), the Gerhard Schmidt Minerva Centre for Supramolecular Chemistry (D.C.), the Kimmel Centre for Nanoscale Science (D.C.), and the Ilse Katz Centre for Materials Research (M.S., D.C.) is gratefully acknowledged. M.S. holds the Katzir-Makineni professorial chair in chemistry, and D.C. holds the Sylvia and Rowland Schaefer chair in Energy Research.

Supporting Information Available: Text, figures, and a table giving the height of fused bR vesicles and of Az and BSA molecules in diluted monolayers, *I*−*V* characteristics of the bare SiO_x substrate, of Br-terminated and SH-terminated substrates, and of BSA on Br-terminated and NH_2-terminated substrates, *I*−*V* characteristics of Az and bR with the two top contacting methods, electrical transport characteristics of the monolayers, AFM images and optical thickness of wild-type bR, Apo-bR, washed Apo-bR, Az, Apo Az, and Zn-Az, and a discussion of the optical thickness of the protein monolayers (ellipsometry values) and of compressional effects by the top contacts on bR. This material is available free of charge via the Internet at http://pubs.acs.org.

JA907328R

(55) McMillin, D. R.; Rosenberg, R. C.; Gray, H. B. *Proc. Natl. Acad. Sci. U.S.A.* **1974**, *71* (12), 4760–4762.